

# Natural Convection in a Cavity with Fins Attached to Both Vertical Walls

George N. Facas\*

Trenton State College, Trenton, New Jersey, 08650

Numerical calculations are presented for two-dimensional natural convection flow inside an air-filled cavity with fins/baffles—of length 0.1, 0.3, and 0.5 of the cavity width—attached along both the heated and the cooled side of the cavity. The governing equations in the stream function-vorticity formulation are solved using finite differences. The Arakawa differencing scheme is used to represent the convection terms. Flow characteristics are investigated for three baffle lengths and Grashof numbers in the range of  $9.0 \times 10^3$  to  $1.0 \times 10^5$ . A multicellular flow structure is found to exist for a baffle length of 0.1. However, when the baffle length is equal to 0.3 or greater, the fluid flow breaks down into secondary circulations—in addition to the primary circulation—and that, in turn, results in higher heat transfer rates across the two sides of the cavity.

## Nomenclature

$Gr$	= Grashof number, $g\beta\Delta Tw^3/\nu^2$
$h$	= baffle length
$N$	= number of baffles
$Pr$	= Prandtl number, $\nu/\alpha$
$T$	= temperature
$u'$	= nondimensional velocity in $\xi$ direction
$v'$	= nondimensional velocity in $\zeta$ direction
$w$	= cavity width
$z$	= cavity length
$\alpha$	= thermal diffusivity
$\beta$	= coefficient of thermal expansion
$\delta$	= baffle thickness
$\xi$	= nondimensional spatial coordinate
$\Theta$	= nondimensional temperature
$\lambda$	= cavity aspect ratio, $z/w$
$\nu$	= kinematic viscosity
$\xi$	= nondimensional spatial coordinate
$\tau$	= nondimensional time
$\Psi$	= nondimensional stream function
$\psi$	= stream function
$\Omega$	= nondimensional vorticity
$\omega$	= vorticity

## Introduction

NATURAL convection in long enclosures has received much attention because of its many engineering applications which include double-pane windows, solar collectors, double-wall insulation, and nuclear reactor insulation. Two excellent comprehensive review articles on the subject have been written by Catton<sup>1</sup> and Ostrach.<sup>2</sup>

It is generally known that for a vertical cavity heated on one side and cooled on the opposite side, the fluid flow is characterized by a single large cell; the fluid ascends along the hot wall, descends along the cold wall, and turns at the opposite ends of the cavity. For small Grashof numbers the flow is weak and the isotherms are parallel to the vertical walls. In this region heat is transferred by conduction across the fluid. This flow regime was first analyzed by Batchelor,<sup>3</sup> who named it the conduction regime. With increasing Grashof number, however, this flow becomes unstable. Hart<sup>4</sup> and Korpela et al.<sup>5</sup> showed that the instability takes different forms

depending on the fluid Prandtl number. In the limit of zero Prandtl number, the instability is purely hydrodynamic and leads to transverse cells. For large Prandtl numbers the instability takes the form of traveling waves. Experiments performed by Elder,<sup>6</sup> using water to visualize the boundary layers along the vertical walls, have shown the presence of secondary stationary motions in the interior of the cavity. These findings have been confirmed by the experimental and numerical studies in Refs. 7–14.

Roux et al.<sup>15</sup> showed that these secondary motions can only be observed in air-filled cavities of aspect ratio greater than a critical value between 11 and 12. Roux et al.<sup>15</sup> have also shown that as the Grashof number further increases, the flow structure changes from multicellular to monocellular and it becomes one of a boundary-layer type. Facas<sup>16</sup> showed that for an air-filled vertical cavity with an aspect ratio of 15 (defined as the ratio of the cavity height to the cavity width) the value of  $Gr$  at which the flow undergoes the transition to monocellular flow depends on the initial condition which is specified. However, based on the cases considered by Facas, monocellular flow has been predicted for  $Gr \geq 4.5 \times 10^4$ .

In the present study, the effect of baffle length and baffle orientation on two-dimensional laminar natural convection inside a long cavity is investigated numerically. The geometry considered is shown in Fig. 1. It is assumed that the left wall is heated to a constant temperature  $T_1$ , whereas the right wall is cooled to a constant temperature  $T_2$ . Both the top and bottom horizontal surfaces are assumed to be adiabatic. In view of the complexity and the large number of parameters involved in this problem, the present study was restricted to cavities with an aspect ratio of 15 and a fluid Prandtl number

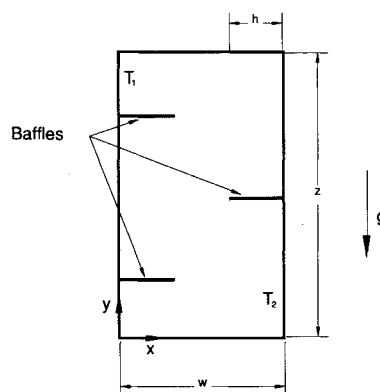


Fig. 1 Geometry and configuration.

Received Aug. 3, 1992; revision received Dec. 27, 1992; accepted for publication Dec. 31, 1992. Copyright © 1992 by the American Institute of Aeronautics and Astronautics, Inc. All rights reserved.

\*Assistant Professor, Mechanical Engineering. Member AIAA.

of 0.71. Three baffle lengths were considered: 1)  $h/w = 0.1$ , 2) 0.3, and 3) 0.5. Results have been obtained for Grashof numbers ranging from  $9.0 \times 10^3$  to  $1.0 \times 10^5$ . For understanding purposes only, if the cavity width is assumed to be 2.5 cm, Grashof numbers ranging from  $9.0 \times 10^3$  to  $1.0 \times 10^5$  would correspond to temperature differences ranging from approximately 5 to 50°C.

### Mathematical Formulation

Consider the two-dimensional cavity of width  $w$  and height  $z$  which contains a Newtonian fluid, as shown schematically in Fig. 1. The problem is to find the velocity and temperature profile inside the cavity, as well as the rate of heat transfer across the two vertical walls, assuming that one of the walls is heated to a constant temperature  $T_1$ , while the other is cooled to constant temperature  $T_2$ .

For natural convection flows it is common to employ the Boussinesq approximation, i.e., to assume that the effect of temperature on density is confined only to the body force term of the momentum equation and that all other fluid properties are independent of temperature and pressure. This implies that the fluid is incompressible, and its equation of state is

$$\rho = \rho_0[1 - \beta(T - T_0)] \quad (1)$$

where  $\rho$  and  $\beta$  represent the density and volumetric expansion coefficient, respectively, and the subscript denotes some reference state.

Using the stream function-vorticity approach, the governing equations with the Boussinesq approximation for two-dimensional incompressible laminar-free convection in dimensionless form are<sup>16</sup>

Stream function equation

$$\frac{\partial^2 \Psi}{\partial \xi^2} + \frac{1}{\lambda^2} \frac{\partial^2 \Psi}{\partial \zeta^2} = -\Omega \quad (2)$$

Vorticity equation

$$\frac{\partial \Omega}{\partial \tau} + u' \frac{\partial \Omega}{\partial \xi} + v' \frac{\partial \Omega}{\partial \zeta} = \left( \frac{\partial^2 \Omega}{\partial \xi^2} + \frac{1}{\lambda^2} \frac{\partial^2 \Omega}{\partial \zeta^2} \right) + Gr \frac{\partial \Theta}{\partial \xi} \quad (3)$$

Energy equation

$$\frac{\partial \Theta}{\partial \tau} + u' \frac{\partial \Theta}{\partial \xi} + v' \frac{\partial \Theta}{\partial \zeta} = \frac{1}{Pr} \left( \frac{\partial^2 \Theta}{\partial \xi^2} + \frac{1}{\lambda^2} \frac{\partial^2 \Theta}{\partial \zeta^2} \right) \quad (4)$$

where

$$Gr = \frac{g\beta(T_1 - T_2)w^3}{\nu^2}, \quad \lambda = \frac{z}{w}, \quad Pr = \frac{\nu}{\alpha}$$

$$x = w\xi, \quad y = z\zeta, \quad \psi = \nu\Psi, \quad \omega = \frac{\nu}{w^2} \Omega$$

$$\Theta = \frac{T - T_2}{T_1 - T_2}, \quad t = \frac{w^2}{\nu} \tau$$

Note that

$$\begin{aligned} u' &= \frac{1}{\lambda} \frac{\partial \Psi}{\partial \zeta} \\ v' &= -\frac{1}{\lambda} \frac{\partial \Psi}{\partial \xi} \end{aligned} \quad (5)$$

The energy equation for the fin has been derived assuming negligible thermal resistance across the thickness of the fin,

negligible capacitance, and a fin thermal conductivity equal to the fluid thermal conductivity. Thus, for the fin

$$\lambda^2 \left( \frac{\delta}{z} \right) \frac{\partial^2 \Theta}{\partial \xi^2} + \left( \frac{\partial \Theta}{\partial \zeta} \right)_2 - \left( \frac{\partial \Theta}{\partial \zeta} \right)_1 = 0 \quad (6)$$

The last two terms represent heat exchange between the fluid and the upper and lower fin surfaces, respectively. The analysis was restricted to a dimensionless baffle thickness of  $\frac{1}{150}$ .

The assumption of a fin thermal conductivity being equal to the fluid thermal conductivity cannot be duplicated in practice even with the best solid insulating materials. Typically, the thermal conductivity of solids is many orders of magnitude larger than the thermal conductivity of a fluid. As a result, the assumption of a fin thermal conductivity being equal to the fluid thermal conductivity represents an extreme limiting case. However, based on the data presented by Winters,<sup>17</sup> it is expected that the results obtained for the extreme case of equal baffle and fluid thermal conductivity are also accurate for higher relative thermal conductivity ratios.

In the dimensionless coordinates the computational domain extends in both directions from 0 to 1. The solution to Eqs. (2–4) with the appropriate boundary conditions yields the desired distribution for  $\Psi$ ,  $\Omega$ , and  $\Theta$ .

### Boundary Conditions

The no-slip condition at the walls,  $u = v = 0$ , yields  $\Psi = \text{const}$ . Thus, the value  $\Psi = 0$  is arbitrarily assigned at all four walls. The vorticity at the walls were calculated using the following second-order accurate expressions:

$$\Omega = \frac{\Psi_{w+2} - 8\Psi_{w+1} + 7\Psi_w}{\lambda^2 \Delta \zeta^2} \quad \zeta = 0, 1 \quad (7a)$$

$$\Omega = \frac{\Psi_{w+2} - 8\Psi_{w+1} + 7\Psi_w}{\Delta \xi^2} \quad \zeta = 0, 1 \quad (7b)$$

Constant uniform temperatures  $T_1$  and  $T_2$  ( $T_1 > T_2$ ) are imposed at the left and right walls, respectively. The top and bottom walls are assumed to be adiabatic. Thus

$$\Theta = 1 \quad \xi = 0, \quad \Theta = 0 \quad \xi = 1$$

$$\frac{\partial \Theta}{\partial \zeta} = 0 \quad \zeta = 0, 1 \quad (8)$$

A second-order accurate finite difference expression was used to evaluate the temperature boundary condition on the insulated walls.

### Method of Solution

The system of equations with the boundary conditions is solved using finite differences. The Arakawa's differencing scheme<sup>18</sup> is used with the convective terms, and central differences are used with the diffusive terms. The Arakawa's scheme was selected for this problem because it has been demonstrated that it can predict the multicellular flow structure that exists in this problem, see Korpela et al.,<sup>8</sup> Lee and Korpela,<sup>9</sup> and Facas.<sup>16</sup> First-order accurate forward differences were used with the time derivatives.

The computer code was validated by comparing average Nusselt number with published results for a vertical cavity without baffles. The results obtained with this computer code are in excellent agreement with the highly accurate numerical solution presented by Ramanan and Korpela.<sup>20</sup> Using a uniform grid mesh of  $51 \times 151$ , the average Nusselt number obtained at  $Gr = 11.85 \times 10^3$  was 0.21% lower than the value presented by Ramanan and Korpela; a 0.43% difference in  $Nu$  relative to the Ramanan and Korpela solution was found at  $Gr = 29.63 \times 10^3$ . Based on these comparisons, a uniform

grid mesh of  $51 \times 151$  appeared sufficient to obtain solutions for the entire range of Grashof numbers considered. The local Nusselt numbers at the two vertical walls were calculated using three-point derivatives. The average Nusselt number was determined from the local  $Nu$  values using Simpson's rule.

All calculations were made using a  $51 \times 151$  uniform grid mesh. The time step used varied from  $1 \times 10^{-4}$  to  $3 \times 10^{-4}$  depending on the value of the Grashof number considered. The solution to the algebraic system of equations at the end of each time step has been obtained using the modified strongly implicit procedure, Schneider and Zedan.<sup>19</sup> The steady-state solution was assumed to have been reached when the residual between time steps was less than  $10^{-4}$  for all three variables at every grid point. Typically, when this criterion was met, the average residual between time steps for the temperature field was in the order of  $10^{-9}$ , whereas the average residual for the stream function and vorticity fields were in the order of  $10^{-6}$  and  $10^{-5}$ , respectively. All computations were carried out on a 386 personal computer.

### Results and Discussion

In a long vertical cavity without baffles, the fluid ascends along the heated surface and descends along the cooled surface (primary circulation). Facas<sup>16</sup> showed that for an air-filled cavity with an aspect ratio of 15, a hydrodynamic instability occurs, in the form of transverse rolls, for Grashof numbers in the range of  $1.2 \times 10^4$  to  $4.0 \times 10^4$ . For  $Gr$  values outside of this range, the flow is characterized by one large cell.

When one baffle of dimensionless length 0.1 is attached midway along the heated side of the cavity there is little effect on the heat transfer and fluid flow structure. The values that were obtained for the local Nusselt number and the average Nusselt number are almost identical to those obtained by Facas<sup>16</sup> for natural convection flow in a differentially heated vertical cavity of aspect ratio 15. Moreover, the qualitative results presented by Facas<sup>21</sup> in the form of streamlines and isotherms show that the presence of one baffle of length 0.1 has little effect on the flow structure; a multicellular flow structure is predicted for Grashof numbers in the range of  $9.0 \times 10^3$  to  $5.0 \times 10^4$  and; a monocellular structure at a  $Gr$  value of  $1.0 \times 10^5$ . A similar fluid flow structure was predicted for a vertical cavity without any baffles attached along the walls by Facas.<sup>16</sup>

As the baffle size increases to 0.3, the flow is characterized by a primary circulation—consisting of the stream that ascends from the bottom to the top of the hot wall and descends along the cold wall—and two secondary circulations, see Figs. 2 and 3. As the fluid ascends along the hot wall, the baffle

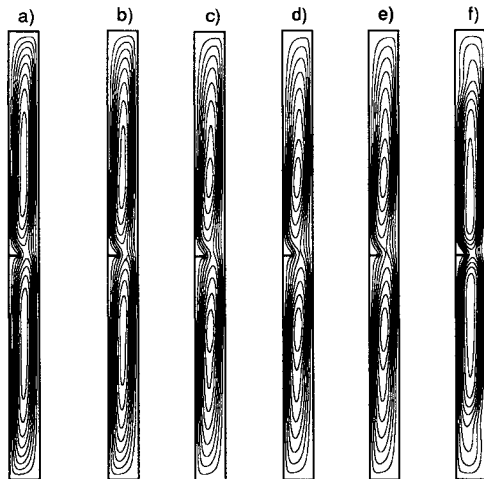


Fig. 2 Streamlines, one baffle along heated wall;  $h/w = 0.3$ : a)  $Gr = 9.0 \times 10^3$ , b)  $Gr = 1.2 \times 10^4$ , c)  $Gr = 2.0 \times 10^4$ , d)  $Gr = 3.0 \times 10^4$ , e)  $Gr = 4.0 \times 10^4$ , and f)  $Gr = 1.0 \times 10^5$ .

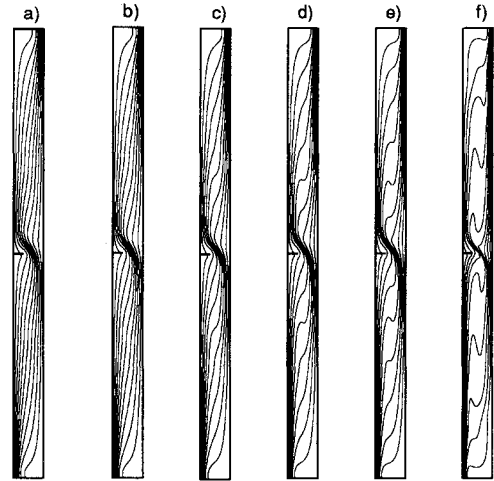


Fig. 3 Isotherms, one baffle along heated wall;  $h/w = 0.3$ : a)  $Gr = 9.0 \times 10^3$ , b)  $Gr = 1.2 \times 10^4$ , c)  $Gr = 2.0 \times 10^4$ , d)  $Gr = 3.0 \times 10^4$ , e)  $Gr = 4.0 \times 10^4$ , f)  $Gr = 1.0 \times 10^5$ .

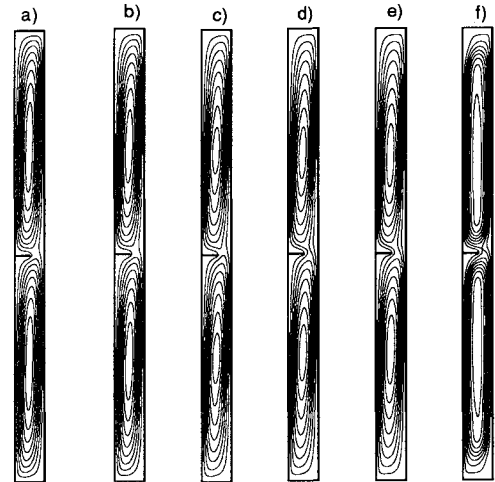


Fig. 4 Streamlines, one baffle along heated wall;  $h/w = 0.5$ : a)  $Gr = 9.0 \times 10^3$ , b)  $Gr = 1.2 \times 10^4$ , c)  $Gr = 2.0 \times 10^4$ , d)  $Gr = 3.0 \times 10^4$ , e)  $Gr = 4.0 \times 10^4$ , f)  $Gr = 1.0 \times 10^5$ .

diverts the fluid flow direction to the right. As a result, the ascending hot stream and the descending cold stream collide and, in this way, two secondary recirculations are established as the strength of the primary flow is weakened. An increase in baffle length to 0.5 reduces further the strength of the primary circulation in favor of stronger secondary flows, see Figs. 4 and 5. The net result of the fluid flow breakdown into one weak primary circulation and two stronger secondary circulations is higher heat transfer rates across the two sides of the cavity, as it is clearly shown by the temperature field (Fig. 5). Essentially, the presence of the baffle tends to reduce the effective cavity aspect ratio which, in turn, yields a higher heat transfer rate across the two vertical sides of the cavity. Figures 3 and 5 show that the temperature field is stratified in the center region of the cavity for the higher  $Gr$  values considered.

The results when two baffles of dimensionless length 0.1 are attached along the heated wall at equal distances are qualitatively similar to those discussed above for one baffle of length 0.1. In short, a multicellular flow structure is predicted up to a  $Gr$  value of  $4.0 \times 10^4$ . However, slight differences are predicted between the one-baffle and two-baffle solution in terms of the  $Gr$  values at which the transition from the four-cell to the three-cell, three-cell to two-cell, and two-cell to one-cell structure occurs. The differences between the two cases considered are discussed in more detail by Facas.<sup>21</sup>

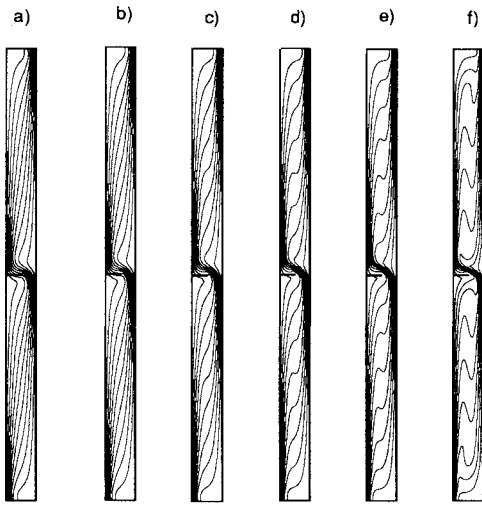


Fig. 5 Isotherms, one baffle along heated wall;  $h/w = 0.5$ : a)  $Gr = 9.0 \times 10^3$ , b)  $Gr = 1.2 \times 10^4$ , c)  $Gr = 2.0 \times 10^4$ , d)  $Gr = 3.0 \times 10^4$ , e)  $Gr = 4.0 \times 10^4$ , f)  $Gr = 1.0 \times 10^5$ .

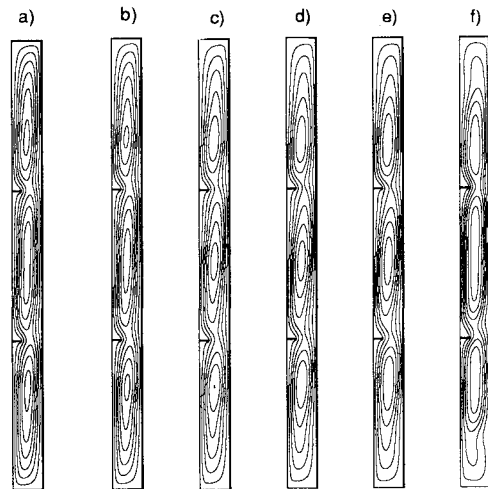


Fig. 6 Streamlines, two baffles along heated wall;  $h/w = 0.3$ : a)  $Gr = 9.0 \times 10^3$ , b)  $Gr = 1.2 \times 10^4$ , c)  $Gr = 2.0 \times 10^4$ , d)  $Gr = 3.0 \times 10^4$ , e)  $Gr = 4.0 \times 10^4$ , f)  $Gr = 1.0 \times 10^5$ .

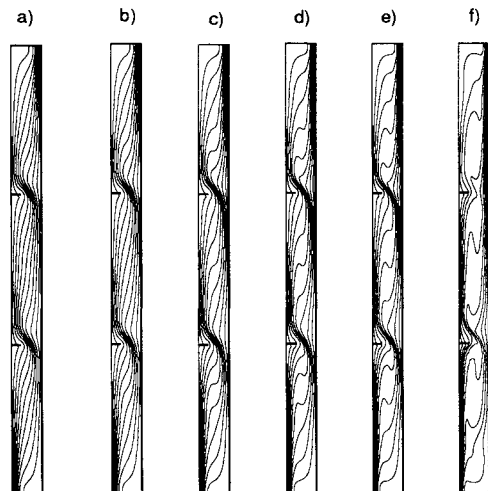


Fig. 7 Isotherms, two baffles along heated wall;  $h/w = 0.3$ : a)  $Gr = 9.0 \times 10^3$ , b)  $Gr = 1.2 \times 10^4$ , c)  $Gr = 2.0 \times 10^4$ , d)  $Gr = 3.0 \times 10^4$ , e)  $Gr = 4.0 \times 10^4$ , f)  $Gr = 1.0 \times 10^5$ .

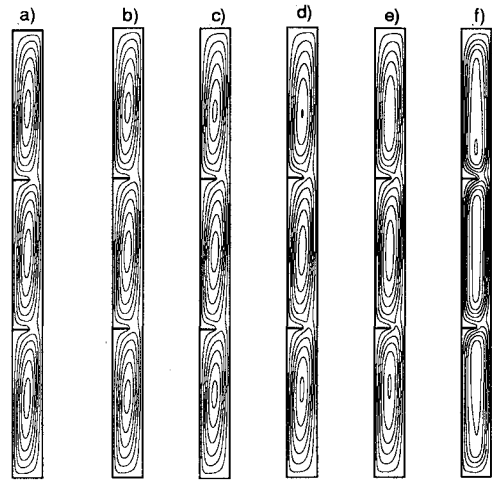


Fig. 8 Streamlines, two baffles along heated wall;  $h/w = 0.5$ : a)  $Gr = 9.0 \times 10^3$ , b)  $Gr = 1.2 \times 10^4$ , c)  $Gr = 2.0 \times 10^4$ , d)  $Gr = 3.0 \times 10^4$ , e)  $Gr = 4.0 \times 10^4$ , f)  $Gr = 1.0 \times 10^5$ .

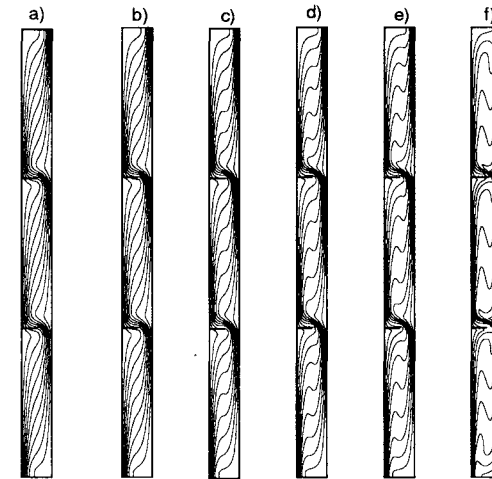


Fig. 9 Isotherms, two baffles along heated wall;  $h/w = 0.5$ : a)  $Gr = 9.0 \times 10^3$ , b)  $Gr = 1.2 \times 10^4$ , c)  $Gr = 2.0 \times 10^4$ , d)  $Gr = 3.0 \times 10^4$ , e)  $Gr = 4.0 \times 10^4$ , f)  $Gr = 1.0 \times 10^5$ .

Figures 6–9 shows results for the stream function and temperature field when two baffles of dimensionless length 0.3 and 0.5 are attached along the heated wall at equal distances. Once again, baffle lengths of 0.3 or greater force the flow to break down into one weak primary—consisting of the stream that ascends from the bottom to the top of the hot wall and descends along the cold wall—and three relatively strong secondary flows. Moreover, with an increase in baffle length from 0.3 to 0.5, the temperature field is stratified in the center region of the cavity even at low  $Gr$  values.

Figures 10 and 11 show results for the stream function and temperature field when baffles of dimensionless length 0.5 are attached on both walls. Attaching one baffle midway along the cooled side of the cavity (in addition to the two baffles attached along the heated side of the cavity at equal distance) causes further breakdowns of the fluid flow into additional secondary circulations. As a result, even higher heat transfer rates are achieved than those which are produced when baffles are attached only on the heated side of the cavity. Given the symmetry in the flow, identical results for the heat transfer would be expected if two baffles were attached along the cooled side and one along the heated side of the cavity.

Figure 12 shows sample results for the local Nusselt number along the heated wall when two baffles are attached along the heated wall and  $Gr = 3.0 \times 10^4$ . As it can be seen, the presence of the baffles of length greater than or equal to 0.3

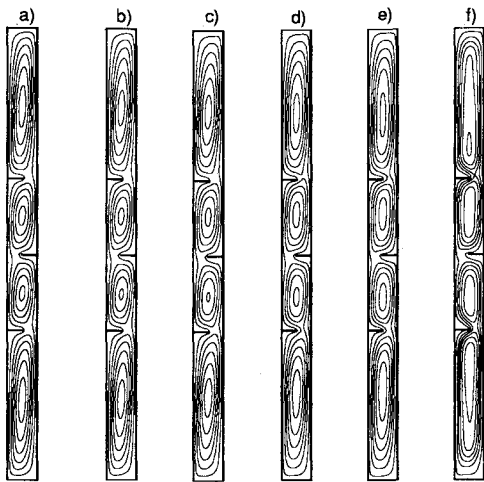


Fig. 10 Streamlines, two baffles along heated wall and one baffle along cooled wall;  $h/w = 0.5$ : a)  $Gr = 9.0 \times 10^3$ , b)  $Gr = 1.2 \times 10^4$ , c)  $Gr = 2.0 \times 10^4$ , d)  $Gr = 3.0 \times 10^4$ , e)  $Gr = 4.0 \times 10^4$ , f)  $Gr = 1.0 \times 10^5$ .

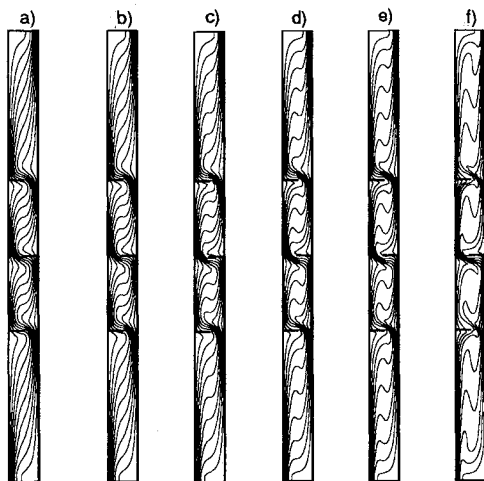


Fig. 11 Isotherms, two baffles along heated wall and one baffle along cooled wall;  $h/w = 0.5$ : a)  $Gr = 9.0 \times 10^3$ , b)  $Gr = 1.2 \times 10^4$ , c)  $Gr = 2.0 \times 10^4$ , d)  $Gr = 3.0 \times 10^4$ , e)  $Gr = 4.0 \times 10^4$ , f)  $Gr = 1.0 \times 10^5$ .

cause large variations on the local Nusselt number. Figure 12 also illustrates that at this  $Gr$  value a baffle length of 0.5 is far more effective from a heat transfer enhancement point of view than a baffle length of 0.3. Furthermore, a comparison of the local Nusselt number results, obtained for a baffle length of 0.1 to the results obtained by Facas<sup>16</sup> for a vertical cavity without any baffles attached, indicate that the impact of the shorter baffles on the local Nusselt number variation is negligible.

Plots of the average Nusselt number as a function of  $Gr$  and number of baffles are shown in Fig. 13 for a baffle length of 0.5. Also shown in Fig. 13 are average Nusselt number results obtained numerically by Facas<sup>16</sup> and Ramanan and Korpela<sup>20</sup> for an air-filled vertical cavity of aspect ratio 15. Figure 13 indicates that the heat transfer rate across the cavity width increases as the number of baffles increases. As an example, when three baffles are attached along the heated and cooled side of the cavity, the heat transfer rate across the two sides of the cavity can increase anywhere from 25 to 10%, depending on the  $Gr$  value being considered. Even when only one baffle of dimensionless length 0.5 is attached along the heated side of the cavity, it still results in a 10% (on the average) heat transfer enhancement for the  $Gr$  range considered.

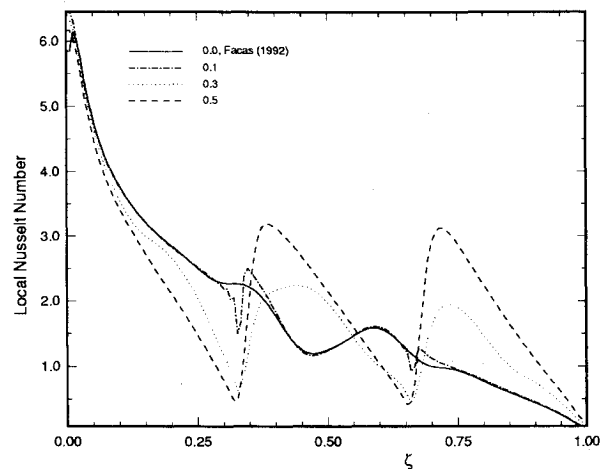


Fig. 12 Local Nusselt number distribution, two baffles along heated wall,  $Gr = 3.0 \times 10^4$ .

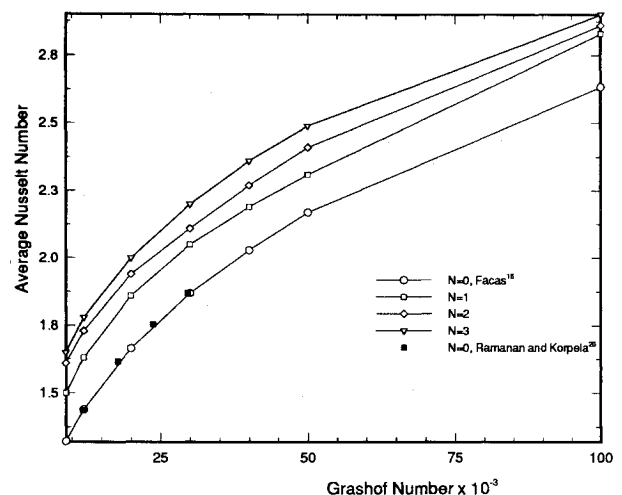


Fig. 13 Average Nusselt number vs. Grashof number and number of baffles,  $h/w = 0.5$ .

## Conclusion

The effect of baffles on the natural convection flow in a long cavity has been analyzed numerically for two-dimensional laminar flow. Flow characteristics have been investigated for three baffle lengths and Grashof numbers up to  $1.0 \times 10^5$ . A multicellular flow structure is found to exist for a baffle length of 0.1. As the baffle length increases to 0.3 or higher, the flow breaks down into secondary circulations and that, in turn, results in higher heat transfer rates across the two sides of the cavity.

## Acknowledgments

This work was partially supported by a FIRSL award administered by Trenton State College. The author would like to express his appreciation to the College.

## References

- 1Catton, I., "Natural Convection in Enclosures," *6th International Heat Transfer Conference*, Toronto, Canada, 1978, pp. 13-31.
- 2Ostrach, S., "Natural Convection in Enclosures," *Journal of Heat Transfer*, Vol. 110, Nov. 1988, pp. 1175-1190.
- 3Batchelor, G. K., "Heat Transfer by Free Convection Across a Closed Cavity Between Vertical Boundaries at Different Temperatures," *Quarterly Journal of Applied Mathematics*, Vol. 12, No. 3, 1954, pp. 209-233.
- 4Hart, J. E., "Stability of the Flow in a Differentially Heated

Inclined Box," *Journal of Fluid Mechanics*, Vol. 47, Pt. 3, 1971, pp. 547-576.

<sup>5</sup>Korpela, S. A., Gozum, D., and Baxi, C. B., "On the Stability of the Conduction Regime of Natural Convection in a Vertical Slot," *International Journal of Heat and Mass Transfer*, Vol. 15, 1973, pp. 1683-1690.

<sup>6</sup>Elder, J. W., "Laminar Free Convection in a Vertical Slot," *Journal of Fluid Mechanics*, Vol. 23, Pt. 1, 1965, pp. 77-98.

<sup>7</sup>Vest, C. M., and Arpaci, V. S., "Stability of Natural Convection in a Vertical Slot," *Journal of Fluid Mechanics*, Vol. 36, Pt. 1, 1969, pp. 1-15.

<sup>8</sup>Korpela, S. A., Lee, Y., and Drummond, J. E., "Heat Transfer Through a Double Pane Window," *Journal of Heat Transfer*, Vol. 104, Aug. 1982, pp. 539-544.

<sup>9</sup>Lee, Y., and Korpela, S. A., "Multicellular Convection in a Vertical Slot," *Journal of Fluid Mechanics*, Vol. 126, 1983, pp. 91-121.

<sup>10</sup>Schinkel, W. M. M., "Natural Convection in Inclined Air Filled Enclosures," Ph.D. Dissertation, Univ. of Technology, Delft, The Netherlands, 1980.

<sup>11</sup>Linthorst, S. J. M., Schinkel, W. M. M., and Hoogendoorn, C. J., "Flow Structure with Natural Convection in Inclined Air-Filled Enclosures," *Journal of Heat Transfer*, Vol. 103, Aug. 1981, pp. 535-539.

<sup>12</sup>Lauriat, G., and Desrayaud, G., "Natural Convection in Air-Filled Cavities of High Aspect Ratios: Discrepancies Between Experimental and Theoretical Results," American Society of Mechanical Engineers Paper 85-HT-37, 1985.

<sup>13</sup>Pignatelli, J. F., and Marcillat, J. F., "Transition to Time-Dependent Free Convection in an Inclined Air Layer," *International Journal of Heat and Fluid Flow*, Vol. 7, No. 3, 1986, pp. 169-178.

<sup>14</sup>Le Quere, P., "A Note on Multiple and Unsteady Solutions in Two-Dimensional Convection in a Tall Cavity," *Journal of Heat Transfer*, Vol. 112, Nov. 1990, pp. 965-974.

<sup>15</sup>Roux, B., Grondin, J., Bontoux, P., and de Vahl Davis, G., "Reverse Transition from Multicellular to Monocellular Motion in a Vertical Fluid Layer," *Proceedings of the Physico Chemical Hydrodynamics Conference*, Vol. 3F, Madrid, European Physical Society, 1980, pp. 292-297.

<sup>16</sup>Facas, G. N., "Laminar Free Convection in a Nonrectangular Inclined Cavity," *Journal of Thermophysics and Heat Transfer*, Vol. 7, No. 3, 1993, pp. 447-453.

<sup>17</sup>Winters, K. H., "The Effect of Conducting Divisions on the Natural Convection of Air in a Rectangular Cavity with Heated Side Walls," American Society of Mechanical Engineers Paper 82-HT-69, 1982.

<sup>18</sup>Arakawa, A., "Computational Design for Long-Term Numerical Integration of the Equations of Fluid Motion: Two-Dimensional Incompressible Flow. Part I," *Journal of Computational Physics*, Vol. 1, 1966, pp. 119-143.

<sup>19</sup>Schneider, G. E., and Zedan, M., "A Modified Strongly Implicit Procedure for the Numerical Solution of Field Problems," *Numerical Heat Transfer*, Vol. 4, 1981, pp. 1-19.

<sup>20</sup>Ramanan, N., and Korpela, S. A., "Multigrid Solution of Natural Convection in a Vertical Slot," *Numerical Heat Transfer*, Pt. A, Vol. 15, 1989, pp. 323-339.

<sup>21</sup>Facas, G. N., "Natural Convection in a Cavity with Fins Attached to Both Vertical Walls," *Natural Convection in Enclosures, Proceedings of the 28th National Heat Transfer Conference*, San Diego, CA, American Society of Mechanical Engineers HTD-Vol. 198, 1992, pp. 1-8.

## Progress in Astronautics and Aeronautics

# Gun Muzzle Blast and Flash

Günter Klingenberg and Joseph M. Heimerl

The book presents, for the first time, a comprehensive and up-to-date treatment of gun muzzle blast and flash. It describes the gas dynamics involved, modern propulsion systems, flow development, chemical kinetics and reaction networks of flash suppression additives as well as historical work. In addition, the text presents data to support a revolutionary viewpoint of secondary flash ignition and suppression.

The book is written for practitioners and novices in the flash suppression field: engineers, scientists, researchers, ballisticians, propellant designers, and those involved in signature detection or suppression.

1992, 551 pp, illus, Hardback, ISBN 1-56347-012-8,  
AIAA Members \$65.95, Nonmembers \$92.95  
Order #V-139 (830)

Place your order today! Call 1-800/682-AIAA



American Institute of Aeronautics and Astronautics  
Publications Customer Service, 9 Jay Gould Ct., P.O. Box 753, Waldorf, MD 20604  
Phone 301/645-5643, Dept. 415, FAX 301/843-0159

Sales Tax: CA residents, 8.25%; DC, 6%. For shipping and handling add \$4.75 for 1-4 books (call for rates for higher quantities). Orders under \$50.00 must be prepaid. Please allow 4 weeks for delivery. Prices are subject to change without notice. Returns will be accepted within 15 days.